PECULIAR PROPERTIES OF SHIP-MOTION GREEN FUNCTIONS IN WATER OF FINITE DEPTH

Xiao-Bo Chen

Bureau Veritas, DTA, 17bis, Place des Reflets, 92400 Courbevoie (France)
Fax: 33-1-4291.3395 Email: xiao-bo.chen@bureauveritas.com

The potential flows generated by a source pulsating with constant frequency and advancing at constant horizontal speed are called ship-motion Green functions as they are involved in the kernel of integral equations established in the ship-motion problems, and include time-harmonic flows with forward speed and the special cases of Neumann-Kelvin steady flow (at zero frequency) and time-harmonic flows without forward speed. Further to an introductory treatise by Chen (1999) in the case of deep water, ship-motion Green functions in water of finite depth is considered here. Based on the formal decomposition of free-surface effects given by Noblesse & Chen (1995), the wave component (dominant in the far field) of ship-motion Green functions expressed as a single integral along the dispersion curves defined in the Fourier plane by the dispersion relation is analyzed. Especially, the peculiar properties of the wave component near the track of the source point located close to or at the free surface are studied by an asymptotic analysis.

1 Ship-motion Green functions in water of finite depth

Under the reference system moving with the source at the speed U along the positive x-axis defined by its (x, y) plane coinciding with the mean free surface and z-axis oriented positively upward, the ship-motion Green functions $G(\vec{\xi}, \vec{x}_s)$ representing the velocity potential of the flow created at a point $\vec{\xi} = (\xi, \eta, \zeta)$ by a pulsating-advancing source of unit strength located at a point $\vec{x}_s = (x_s, y_s, z_s)$, can be expressed as

$$G = G^S + G^F \tag{1}$$

where G^F accounts for free-surface effects and G^S is defined in terms of simple singularities

$$4\pi\, G^S = \sum_{n=-\infty}^{\infty} (-1)^n \left\{ -1/\sqrt{r^2 + (\zeta - z_s + 2nh)^2} + 1/\sqrt{r^2 + (\zeta + z_s + 2nh)^2} \right\} \tag{2}$$

in which $r = \sqrt{(\xi - x_s)^2 + (\eta - y_s)^2}$ and $h = H/L$ is the adimensional waterdepth with respect to the reference length L. The simple part G^S defined by (2) satisfies $G^S = 0$ at the free surface ($\zeta = 0$) and $\partial G^S / \partial \zeta = 0$ at the sea bed ($\zeta = -h$). The free-surface part G^F in (1) is defined by a double integral representing the Fourier superposition of elementary waves

$$4\pi^2 G^F = \lim_{\epsilon \to +0} \int_{-\infty}^{\infty} d\beta \int_{-\infty}^{\infty} d\alpha \, \frac{A\, e^{-i(\alpha x + \beta y)}}{D + i\epsilon\, \mathrm{sign}(D_f)} \tag{3}$$

with $(x, y) = (\xi - x_s, \eta - y_s)$ and A defined by

$$A = \cosh k(\zeta + h) \cosh k(z_s + h) / \cosh^2 kh \quad \text{with} \quad k = \sqrt{\alpha^2 + \beta^2} \tag{4}$$

Furthermore, the dispersion function D in (3) is given by

$$D = (f - F\alpha)^2 - k \tanh kh \tag{5}$$

in which $f = \omega\sqrt{L/g}$ and $F = U/\sqrt{gL}$ are respectively called adimensional frequency and Froude number, as ω and U stand respectively for wave encounter frequency and ship's speed, and L and g for ship's length (taken as the reference length) and the acceleration of gravity. The function $\mathrm{sign}(D_f)$ is given by

$$\mathrm{sign}(D_f) = \mathrm{sign}(\partial D / \partial f) = \mathrm{sign}(f - F\alpha) \tag{6}$$

Following the analysis by Noblesse & Chen (1995), the free-surface part G^F can be decomposed as $G^F = G^W + G^N$ with G^W the wave component and G^N the nonoscillatory component negligible in the far field. The wave component is defined by the single Fourier integral along the dispersion curves defined by the dispersion relation $D = 0$

$$4\pi\, G^W = -i \sum_{D=0} \int_{D=0} ds \, (\Sigma_1 + \Sigma_2) e^{-i(\alpha x + \beta y)} A / \|\nabla D\| \tag{7}$$

where $\sum_{D=0}$ means summation over all the dispersion curves and ds is the differential element of arc length of a dispersion curve. The function $\Sigma_1 = \text{sign}(D_f)$ is associated with the limit $\epsilon \to +0$ in (3) and ensures the satisfaction of the radiation condition, while the sign function Σ_2 is given in [2]

$$\Sigma_2 = \text{sign}(xD_\alpha + yD_\beta) \quad \text{with} \quad (D_\alpha, D_\beta) = (\partial D/\partial\alpha, \partial D/\partial\beta) \tag{8}$$

and used in the following analysis.

2 Dispersion relation and far-field waves

The dispersion function D defined by (5) is associated with the boundary condition on the free surface of wave diffraction-radiation with forward speed in water of finite depth. The dispersion relation $D = 0$ can be written as

$$(\tau - a)^2 - c\tanh(c/F_h^2) = 0 \quad \text{with} \quad \tau = fF \quad \text{and} \quad F_h = U/\sqrt{gH} \tag{9}$$

by using the speed-scaled Fourier variables $(a, b, c) = (\alpha, \beta, k)F^2$ and $H = Lh$ the waterdepth.

The equation (9) defines several distinct dispersion curves symmetric with respect to the axis $\beta = 0$ depending on both the value of τ and that of F_h. In deep water ($F_h = 0$), there exist two or three distinct dispersion curves at a value of τ smaller or larger than 1/4. For $\tau < 1/4$, two open dispersion curves are located on the left and right half Fourier planes and one closed dispersion curve in between around the origin, as shown in Fig.1 by solid lines. At $\tau = 1/4$, the left open dispersion curve is connected to the closed dispersion curve. For $\tau > 1/4$, the left open dispersion curve goes on the right half Fourier plane near the origin while the right open dispersion curve keeps its similar form on the right half Fourier plane.

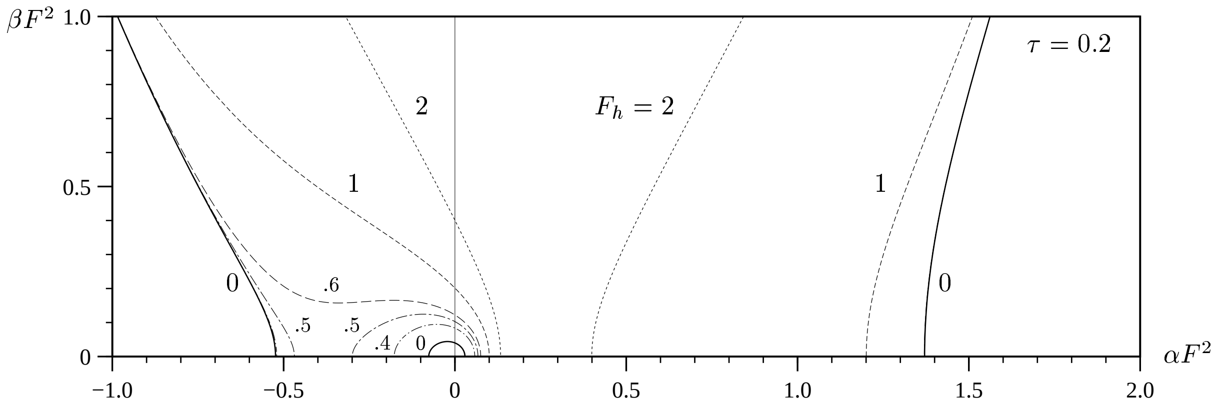

Fig.1 Dispersion curves at $\tau = 0.2$ for various values of F_h

In water of finite depth ($F_h > 0$), the dispersion curves change their form even for a constant value of τ as shown by Fig.1 which depicts the dispersion curves at $\tau = 0.2$ for different values of $F_h = 0, 0.4, 0.5, 0.6, 1$ and 2. The left open dispersion curve and the closed dispersion curve are distinct for small values of F_h and connected to become one open dispersion curve for large values of F_h. The two open dispersion curves at large values of F_h become more and more vertical in the region near the axis $\beta = 0$ and their intersection points with the axis tend to $a = \tau$, i.e. $\alpha = f/F$. An interesting feature of dispersion curves is that the variations of the geometrical form associated with the variation of F_h at a constant $\tau > 0$ are quite similar to those associated with the variation of τ in deep water ($F_h = 0$).

The analysis by Chen & Noblesse (1997) shows that each dispersion curve is related to a wave system, and establishes a direct relationship between the geometrical properties of a dispersion curve and important aspects of the corresponding far-field waves including wavelength, direction of propagation, phase and group velocities and cusp angles. Applying to the case of finite-depth water, we have similar wave systems as in deep water: the inner-V waves are associated with the right open dispersion curve for $F > 0$, the ring waves associated with the closed dispersion curve and the outer-V waves with the left open dispersion curve for small values of both $\tau < 1/4$ and F_h while the partial ring and fan waves appear and are associated with the left open dispersion curve at larger values of F_h even at $\tau < 1/4$. Following the analysis in [4], the transverse and divergent waves associated with the open dispersion curves are respectively corresponding to the part of dispersion curves between two inflection points (symmetrical with respect to $\beta = 0$) and the part from the inflection points to infinity. Unlike the case of steady flows ($\tau = 0$) where the transverse waves disappear for super-critical flows $F_h > 1$, there exist still time-harmonic transverse waves (included in the inner-V wave system) and partial-ring waves (in partial-ring and fan waves) in the downstream for $F_h > 1$.

3 Wave component near the track of a source point

Similar to the analysis in [3] on the wave component of time-harmonic flows in deep water near the track of the source point close to or at the free surface, the asymptotic expansion of the open dispersion curves at large wavenumber is developed first. In fact, the dispersion relation (9) is found to be asymptotically

$$b = -1/2 + \tilde{a}^2 - \tau/\tilde{a} + O(\tilde{a}^{-2}) \quad \text{as} \quad |\tilde{a}| \to \infty \quad \text{with} \quad \tilde{a} = a - \tau \tag{10}$$

in which the first two terms on the right hand side represent a parabola with the axis $a = \tau$ and the vertex located at $(a, b) = (\tau, -1/2)$, and the parameter F_h disappears as the hyperbolic tangent function in (9) tends to the unity exponentially at large values of c. The open dispersion curves at $\tau = 0.2$ are depicted by Fig.2 which shows that all dispersion curves for different values of F_h tend to coincide at large wavenumber.

In (7), the values of $\Sigma_1 = \text{sign}(D_f)$ are equal to ± 1 respectively for the left $(a < a^-)$ and right $(a > a^+)$ open dispersion curves where $a^-(<\tau)$ and $a^+(>\tau)$ are intersection points of the left and right open dispersion curves with the axis $\beta = 0$. At large wavenumber, $|D_\beta/D_\alpha| \approx 0$ along $D = 0$ so that $\Sigma_2 = \text{sign}(xD_\alpha) = \pm 1$ respectively for the left and right open dispersion curves, since we consider $x < 0$ and $y \to 0$ near the track of a source point. Furthermore, the identity

$$ds/\|\nabla D\| = d\alpha/|D_\beta| = F^{-2} da (c/b) C \tag{11}$$

with

$$C = 2\cosh^2(c/F_h^2)/[2c/F_h^2 + \sinh(2c/F_h^2)] \tag{12}$$

valid for any point (a, b) along open dispersion curves can be used in (7) to define the wave component associated with the two open dispersion curves

$$2\pi F^2 G^W = -i\left(\int_{-\infty}^{a^-} - \int_{a^+}^{\infty}\right) AC\,\frac{c}{b}\,(E^+ + E^-)\,da \tag{13}$$

with $E^\pm = \exp(-iXa \pm iYb)$ and $(X, Y) = (x, y)/F^2$

The function A given by (4) can be expressed as

$$A = \frac{\exp(2c/F_h^2)}{4\cosh^2(c/F_h^2)}\left(e^{-cZ_1} + e^{-cZ_2} + e^{-cZ_3} + e^{-cZ_4}\right) \tag{14}$$

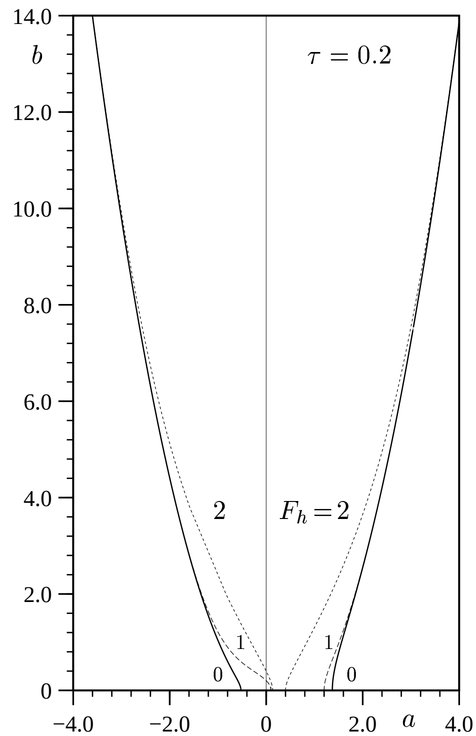

Fig.2 Open dispersion curves

with

$$Z_1 = -(\zeta + z_s)/F^2\,, \quad Z_2 = (\zeta + z_s)/F^2 + 4/F_h^2\,, \quad Z_3 = -(\zeta - z_s)/F^2 + 2/F_h^2\,, \quad Z_4 = (\zeta - z_s)/F^2 + 2/F_h^2 \tag{15}$$

By making use of (10), (12) and (14), the wave component defined by (13) can be expressed as

$$2\pi F^2 G^W = \mathcal{G}_0^W + \mathcal{G}_1^W + \mathcal{G}_R^W \tag{16}$$

in which the first two terms are defined by

$$\mathcal{G}_0^W = -ie^{-i\tau X}\left(\int_{-\infty}^{\tilde{a}^-} - \int_{\tilde{a}^+}^{\infty}\right)\sum_{n=1}^{4}(\mathcal{E}_n^+ + \mathcal{E}_n^-)\,d\tilde{a} \quad \text{and} \quad \mathcal{G}_1^W = \tau Y e^{-i\tau X}\left(\int_{-\infty}^{\tilde{a}^-} - \int_{\tilde{a}^+}^{\infty}\right)\sum_{n=1}^{4}\frac{\mathcal{E}_n^+ - \mathcal{E}_n^-}{\tilde{a}}\,d\tilde{a} \tag{17}$$

with $\mathcal{E}_n^\pm = \exp[-(Z_n \pm iY)\tilde{a}^2 - iX\tilde{a} \pm iY/2]$ where $\tilde{a} = a - \tau$, and the remaining term defined by

$$\mathcal{G}_R^W = \left(\int_{-\infty}^{\tilde{a}^-} - \int_{\tilde{a}^+}^{\infty}\right)\left[O(\tilde{a}^{-2}) + O(e^{-2\tilde{a}^2/F_h^2})\right]\,d\tilde{a} \tag{18}$$

can be shown to yield a finite and non-oscillatory value near the source's track, since the integrand is absolutely integrable. The terms $\mathcal{G}_0^W$ and $\mathcal{G}_1^W$ defined by (17) can be further expressed by using the complex error function given in Abramowitz & Stegun (1967). By considering the asymptotic behavior of the complex error function obtained in [3], the leading terms of the wave component can be written asymptotically as $Y \to 0$

$$\mathcal{G}_0^W = e^{-i\tau X}\sum_{n=1}^{4}\widetilde{\mathcal{G}_{0n}^W} + O(1) \quad \text{and} \quad \mathcal{G}_1^W = \tau e^{-i\tau X}\sum_{n=1}^{4}\widetilde{\mathcal{G}_{1n}^W} + O(1) \tag{19}$$

$$\text{with}\quad \widetilde{\mathcal{G}_{0n}^W} = \frac{e^{-Z_n X^2/(4R_n^2)}}{\sqrt{R_n/\pi}/2}\sin\left(\frac{\theta_n - Y}{2} - \frac{X^2 Y}{4R_n^2}\right) \quad\text{and}\quad \widetilde{\mathcal{G}_{1n}^W} = -i\frac{4Ye^{-Z_n X^2/(4R_n^2)}}{X\sqrt{1/(\pi R_n)}}\cos\left(\frac{\theta_n + Y}{2} + \frac{X^2 Y}{4R_n^2}\right) \quad (20)$$

in which the notations $R_n = \sqrt{Z_n^2 + Y^2}$ with Z_n defined by (15) and $\theta_n = \arctan(Y/Z_n)$ are used.

In summary, the wave component near the track of a pulsating-advancing source is expressed as

$$2\pi F^2 G^W = \widetilde{\mathcal{G}^W} + \widetilde{\mathcal{G}_R^W} \quad\text{with}\quad \widetilde{\mathcal{G}^W} = e^{-i\tau X}\left(\sum_{n=1}^{4}\widetilde{\mathcal{G}_{0n}^W} + \tau\sum_{n=1}^{4}\widetilde{\mathcal{G}_{1n}^W}\right) \tag{21}$$

in which the principal part $\widetilde{\mathcal{G}^W}$ is defined with the leading terms given by (20) and the remaining part $\widetilde{\mathcal{G}_R^W} = 2\pi F^2 G^W - \widetilde{\mathcal{G}^W}$ is finite with a magnitude of order $O(1)$ and non-oscillatory with respect to Y. The leading terms $\widetilde{\mathcal{G}_{0n}^W}$ and $\widetilde{\mathcal{G}_{1n}^W}$ are highly-oscillatory as $Y \to 0$ due to the term $X^2Y/(4R_n^2)$ in the trigonometric functions which associates Y with an increasing wavenumber $X^2/(4R_n^2)$ for small R_n especially as $R_1 \to 0$ (when $Y \to 0$ and $Z_1 \to 0$). Furthermore, the leading term $\widetilde{\mathcal{G}_{01}^W}$ is singular near the track as $Y \to 0$ of the source located at the free surface ($Z_1 = 0$).

4 Discussions and conclusions

The singular and highly-oscillatory properties of ship-motion Green functions in water of finite depth represented by $\widetilde{\mathcal{G}^W}$ in (21) are illustrated in Fig.3 for a source point located at the free surface (left part) and for an immerged source point close to the free surface (right part) at $\tau = 0.2$ and $F_h = 1$ along $X = -5$. The real and imaginary parts are depicted respectively by the solid and dashed lines. This result can be considered as an extension of the study in [3] on deep-water Green functions to the more general case of finite-depth water. Furthermore, the formulations developed in [1] in deep-water case are useful in developing formulations for finite-depth Green functions since they possess similar properties.

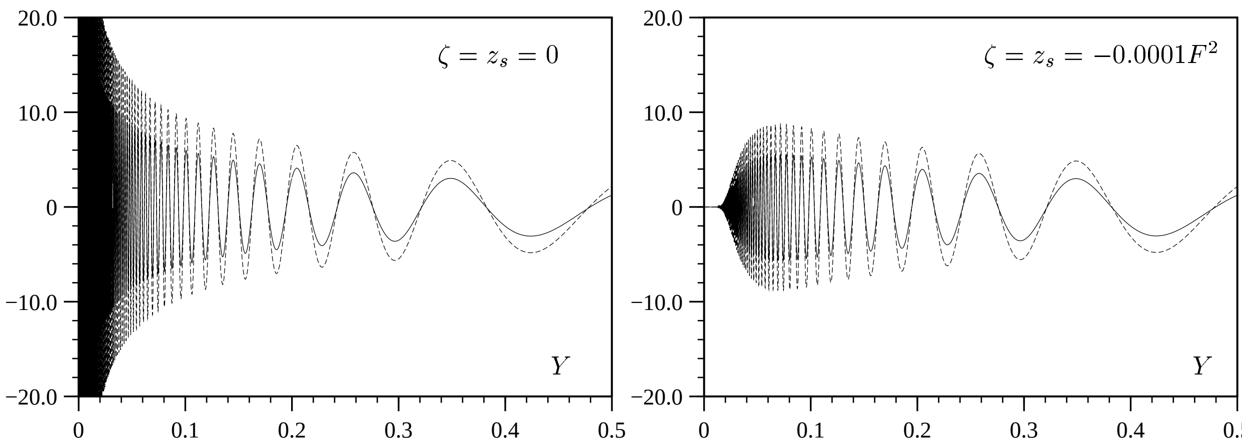

Fig.3 Wave component near the track of a source at the free surface (left) and an immerged source (right)

These peculiar properties of ship-motion Green functions indicate that usual panel methods based on a constant or linear distribution of sources and dipoles may not be reliable since the waterline integral carried out by numerical quadrature cannot be accurate, due to dramatic cancellations of highly-oscillatory values. The new results obtained in the present study are critically important in understanding all aspects of free-surface dispersive flows and very useful in providing a robust and consistent method based on a higher-order distribution of singularities and analytical integrations of the singular and highly-oscillatory terms such as studied in [6], to solve 3D ship-motion problems in a fully satisfactory way.

References

[1] Chen X.B. 1999 An introductory treatise on ship-motion Green functions. *Proc. 7th Intl Conf. on Num. Ship Hydro. Nantes (France)*, 1-21.

[2] Noblesse F. & Chen X.B. 1995 Decomposition of free-surface effects into wave and near-field components. *Ship Tech. Res.* 42, 167-185.

[3] Chen X.B. 1998 On singular and highly-oscillatory properties of ship-motion Green functions.

[4] Chen X.B. & Noblesse F. 1997 Dispersion relation and far-field waves. *12th IWWWFB.*

[5] Abramowitz M. & Stegun I.A. 1967 Handbook of mathematical functions. *Dover Publications.*

[6] Doutreleau Y. & Chen X.B. 1999 Line integrals on the free surface in ship-motion problems. *14th IWWWFB.*